Probing a two-dimensional Fermi surface by tunneling

J. P. Eisenstein, T. J. Gramila, L. N. Pfeiffer, and K. W. West
AT&T Bell Laboratories, Murray Hill, New Jersey 07974
(Received 11 April 1991)

Equilibrium tunneling between parallel two-dimensional electron systems is measured as a function of in-plane magnetic field and sheet density. For equal two-dimensional densities the tunnel conductance is sharply peaked around zero field, but varies slowly at intermediate fields. Around 6 T the conductance exhibits a weaker peak followed by an abrupt drop to zero. A simple model of two displaced, but intersecting, Fermi circles explains these results.

The tunneling conductance between two purely two-dimensional electron systems (2DEG) in semiconductor heterostructures has only recently become experimentally accessible.[1-3] This contrasts with the extensive study[4-7] of 3D-2D systems, a notable example of which is the double-barrier resonant tunneling structure. The main obstacle presented by the 2D-2D problem is the difficulty of producing separate electrical connection to two thin conducting layers separated by typically only 100 Å. Measurements of the 2D-2D tunneling conductance can, however, provide information on 2D systems complementary to that obtained from conventional transport studies. Recent examples include evidence for momentum nonconservation upon tunneling[1] and the observation of field-induced resonant tunneling peaks[3] with large peak-to-valley ratios.

At zero magnetic field the tunneling between 2D systems is highly constrained by energy and momentum conservation. With complete momentum conservation, tunneling can proceed only if the subband edges of the two quantum wells are closely aligned. This follows because, in contrast to the 3D-2D case, conserved in-plane momentum implies conserved kinetic energy. Thus the subband edges must match for total energy to be conserved upon tunneling. For equilibrium tunneling (i.e., nearly equal chemical potentials) between 2DEG's, this is equivalent to requiring matched densities. Using a gate technique, Eisenstein, Pfeiffer, and West[3] observed narrow tunneling peaks at equal 2D densities (within experimental uncertainty), suggesting a high degree of momentum conservation.

In the present work, the tunneling conductance between two 2DEG's confined in quantum wells separated by a thin barrier is investigated as a function of a magnetic field applied parallel to the 2D planes. The conductance is measured without an applied dc bias and thus represents equilibrium tunneling of electrons at the Fermi surfaces of the 2DEG's. With an in-plane magnetic field, conservation of *canonical* momentum no longer implies kinetic-energy conservation and the singular nature of the tunneling is relaxed. An elementary model is proposed that reveals the field dependence of the tunneling to be a map of the Fermi surface. In effect, the magnetic field displaces the origins of the two Fermi seas and allows a sweep of one past the other.

The sample employed here is a modulation-doped double-quantum-well (DQW) structure grown by molecular-beam epitaxy. Two 140-Å-wide GaAs wells separated by an undoped 70-Å AlAs barrier are embedded in the alloy $Al_{0.3}Ga_{0.7}As$. Si doping layers placed above and below the DQW populate the lowest subband of each quantum well with a 2DEG of nominal density[8] 1.5×10^{11} cm^{-2} and low temperature mobility 8×10^{5} $cm^2/V\,s$, these parameters being determined by magneto-transport studies on the individual 2DEG's. While the exact densities of the 2DEG's vary slightly upon thermal cycling (by a few percent), the two wells are matched to within 10%.

A bar-shaped mesa, 50 μm wide in its central region, is defined on the sample top surface by standard photolithographic techniques. The inset to Fig. 1(a) presents a longitudinal cross section through the sample. The magnetic field is applied perpendicular to the long axis of the mesa and parallel (to within 0.5°) to the 2D planes. Diffused indium Ohmic contacts are made at the two ends of the bar. These contacts connect to both 2DEG's simultaneously. Four aluminum Schottky gates are deposited so as to straddle the mesa. Before the two back gates are made, the entire sample is thinned to about 55 μm by chemically removing most of the substrate. The two gates closest to the contacts, labeled *a* and *b* in the figure, are biased to locally deplete the upper and lower 2DEG's, respectively. As the figure inset illustrates, these depleted regions break all direct connection between the two contacts, in effect creating the separate 2DEG contacts required for direct tunneling studies. In this configuration the conductance between contacts 1 and 2 is dominated by the tunneling resistance through the barrier. This technique for independently contacting closely spaced 2D layers has been described in detail elsewhere.[9] The remaining gates, a 50-μm-wide top gate and a larger back-side gate, are employed to locally alter the upper and lower 2DEG densities, respectively.

The two-terminal conductance $G_{1,2}$ between the contacts is measured using 0.1-mV, 27-Hz excitation. The results reported here were found to be essentially independent of temperature below about $T\sim1.5$ K and excitation voltage below about $V_{ex}\sim0.25$ mV. This excitation level is much smaller than the Fermi energies of the

2DEG's ($E_F \sim 5$ meV). Consequently, the observed conductance results from equilibrium tunneling in the $T=0$ limit; i.e., only electrons at the Fermi level participate. A schematic band diagram of the DQW under tunneling conditions is also contained in Fig. 1(a).

The central experimental results of this paper are also shown in Fig. 1. In Fig. 1(a) the tunneling conductance $G_{1,2}$ at $T=0.3$ K is plotted as a function of the applied in-plane magnetic field B. Both the top and bottom gates in the center of the mesa are grounded. Under these conditions the upper and lower 2DEG's have nearly equal densities, 1.50 and 1.58×10^{11} cm^{-2}, respectively. As Fig. 1(a) reveals, a rapidly falling conductance at low fields is followed by a weak field dependence out to about 5 T. Increasing the field further yields a local maximum and then a sharp drop to zero conductance which extends beyond 10 T.

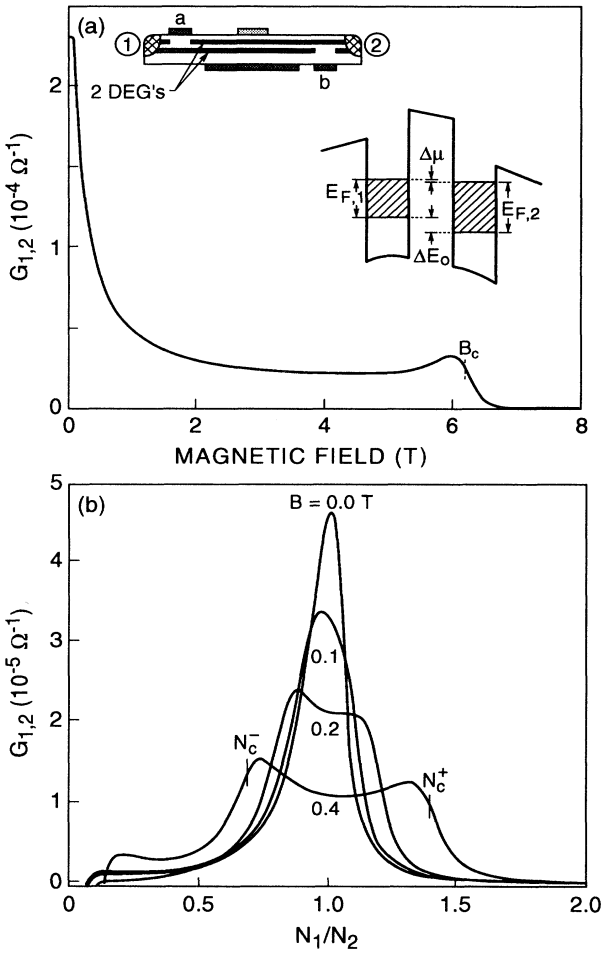

FIG. 1. (a) Tunnel conductance vs magnetic field at $T=0.3$ K. The 2D densities are 1.50 and 1.58×10^{11} cm^{-2} for the upper and lower quantum wells, respectively. The calculated critical field is indicated. Insets depict an idealized cross section through sample, showing Ohmic contacts (hatched) and gates (shaded), and a schematic conduction-band diagram of the DQW. (b) Tunnel conductance vs ratio of upper to lower 2DEG densities at $T=1.3$ K for several magnetic fields. Lower 2DEG density is fixed at about 0.90×10^{11} cm^{-2} while upper 2DEG density is swept by biasing the central top gate. A constant background has been subtracted from each trace. Calculated critical densities are indicated. Features at extreme left are associated with the imminent full depletion of the upper 2DEG.

In Fig. 1(b) the tunneling conductance at $T=1.3$ K is shown as a function of the ratio N_1/N_2 of the upper to lower 2DEG densities for various fixed magnetic fields. These density sweeps are obtained by varying the bias voltage applied to the central top gate; this has a negligible effect on the lower 2DEG density N_2. The conversion between applied gate bias and 2D density is estimated from knowledge of the unbiased densities, the gate capacitance, and the voltages required to fully deplete the individual 2DEG's. As discussed earlier,[3] this method is subject to experimental uncertainties on the order of 15%. We assume, therefore, that the two densities are precisely matched at the peak of the zero-field resonance. As biasing the central top gate affects the tunneling only in the 50×50-μm region under the gate, a background conductance resulting from tunneling elsewhere on the mesa is also present. This background is minimized by applying a fixed bias to the large back-side gate. This unbalances the densities over most of the tunneling region and thereby suppresses the tunneling. The top gate locally restores balance, albeit at a density different from the unbiased condition.[3] For the data in Fig. 1(b), the back-gate bias (-40 V) has reduced the lower 2DEG density to about $N_2\sim0.90\times10^{11}$ cm^{-2}. The residual tunneling background, which depends on magnetic field, has been subtracted to obtain the curves shown.

To understand the data in Fig. 1 we assume the individual quantum wells in the DQW can be treated independently. This amounts to a weak tunneling assumption. For each well the electronic energies are of the form $\varepsilon=E_0+(\mathbf{p}+e\,\mathbf{A})^2/2m$ with E_0 the ground-state energy in the well and $\mathbf{p}$ the in-plane canonical momentum. We take the 2DEG's to lie in the xy plane and the magnetic field $\mathbf{B}$ in the negative y direction. In the Landau gauge the vector potential lies in the x direction and is given by $A_x=-Bz$. The origin of the z axis is taken to be at the center of the upper quantum well, while the center of the lower well lies at $z=+d$; for this sample $d=210$ Å. Treating the magnetic field as a first-order perturbation, the electronic energies ε_1 and ε_2 in the upper and lower quantum wells, respectively, are

$$\begin{aligned}\varepsilon_1&=E_{0,1}+\hbar^2(k_x^2+k_y^2)/2m\ ,\\ \varepsilon_2&=E_{0,2}+\hbar^2[(k_x-k_B)^2+k_y^2]/2m\ .\end{aligned}\tag{1}$$

In these equations $k_B=eBd/\hbar$. An additive diamagnetic contribution to the energies has been omitted; it is the same for both quantum wells and has no relevance here. For $B=0$ it is clear that tunneling with momentum and energy conservation can only occur if $E_{0,1}=E_{0,2}$, i.e., with matched subband edges. Applying an in-plane magnetic field relaxes this condition.

As already discussed, only those electrons at the Fermi surfaces contribute to the observed tunneling current:

i.e., $\varepsilon_1 = E_{0,1} + E_{F,1} \equiv \varepsilon_{1,F}$ and $\varepsilon_2 = E_{0,2} + E_{F,2} \equiv \varepsilon_{2,F}$. A net tunnel current flows in response to the small chemical potential difference $\Delta\mu = eV_{ex}$ imposed by the excitation voltage. Both the measurement temperature and the excitation level were kept small enough to justify an equilibrium, $T = 0$ model of the tunneling.

From Eq. (1) it is apparent that while the Fermi surface of the upper quantum well is a circle centered at the origin in **k** space, that of the lower well is a circle centered at $k_x = k_B$. The radii of these circles are determined by the two densities N_1 and N_2. Tunneling with conserved energy and momentum occurs only at the *intersection* of these circles, as depicted in Fig. 2.

The data in Fig. 1(a) were obtained with nearly equal 2D densities. Thus at $B = 0$ the two Fermi circles have nearly the same diameter (i.e., equal Fermi wave vectors, $k_{F,1} \sim k_{F,2}$) and tunneling occurs all around their perimeters. Only a small magnetic field is required to greatly reduce the tunneling as the region of intersection immediately becomes pointlike due to the relative displacement of the Fermi circles. At intermediate fields the tunneling varies slowly as the two intersection points move around the circle. Approaching $k_B = 2k_F$ leads to enhanced tunneling since the circles are nearly parallel at their intersection point. As k_B exceeds $2k_F$ the tunneling is quenched entirely; the circles no longer overlap at all. Figure 2(a) illustrates these situations, along with numerical results to be discussed. With $N_1 \sim N_2 \sim 1.54 \times 10^{11}$ cm^{-2} the critical magnetic field for quenching the tunneling is $B_c = 2\hbar k_F / ed \sim 6.3$ T, in good agreement with the data in Fig. 1(a).

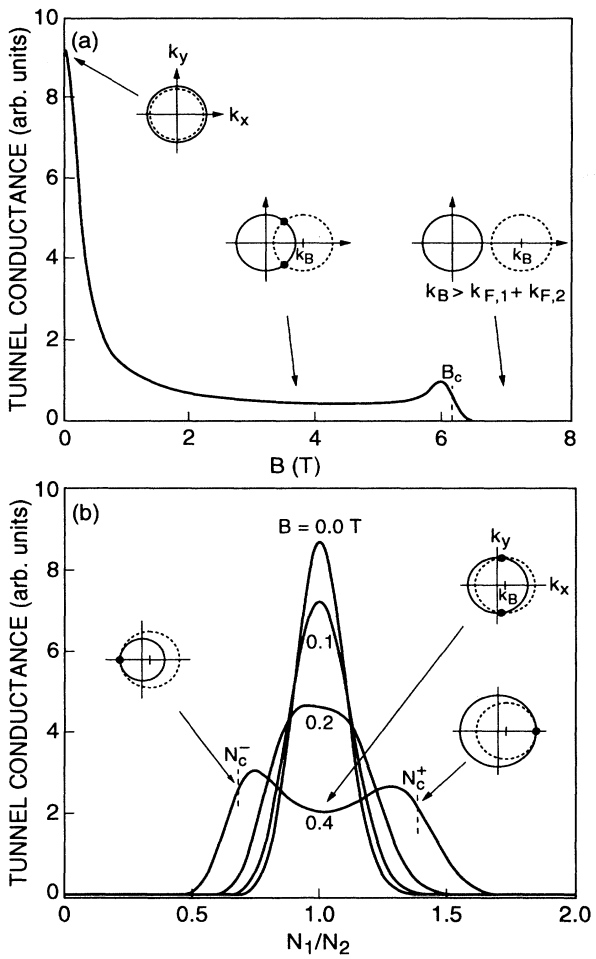

FIG. 2. (a) Calculated tunnel conductance for experimental conditions present in Fig. 1(a). Insets depict relative alignment of Fermi circles for the upper (solid) and lower (dashed) 2DEG. Calculated critical field is indicated. (b) Calculated tunnel conductance vs density ratio N_1/N_2 with N_2 fixed. Conditions appropriate to Fig. 1(b). Calculated critical densities are indicated. Insets depict alignment and relative diameter of Fermi surfaces for representative conditions.

Similar arguments explain the data contained in Fig. 1(b). Now the density of the upper well, N_1, is swept past that of the lower well at various fixed magnetic fields. At zero magnetic field a simple tunneling resonance is observed.[3] The width of the peak ($\sim 15\%$ of the resonant density or Fermi energy) is a measure of how close the Fermi radii must be for significant tunneling, and therefore reflects a breakdown of our assumption of perfect homogeneity and momentum conservation. For a finite magnetic field two critical conditions are expected, as illustrated in Fig. 2(b). The low density cutoff N_c^- of the tunneling occurs when the well 1 circle "kisses" the well 2 circle from the inside while the high density cutoff N_c^+ comes at an outside "kiss." The tunnel resonance is broadened by the in-plane field, with enhancements near the cutoffs. The calculated critical densities agree well with the data, as Fig. 1(b) reveals. Smoliner *et al.*[2] were the first to observe this broadening effect, albeit without evidence for the enhancement near cutoff created by the "kissing" effect.

A more quantitative analysis of the field and density dependence of the tunnel conductance requires assumptions regarding the origin of the width of the $B = 0$ resonance. For definiteness, we adopt a model in which this width is due entirely to elastic scattering. As already noted,[3] the observed width (in energy) is about 10 times larger than $\hbar/\tau$, with τ the mobility lifetime. Conceivably, the substantial difference between large- and small-angle scattering rates characteristic of modulation-doped heterostructures can explain this discrepancy, but other mechanisms, such as well-width fluctuations, may play a larger role. Thus we emphasize that while the scattering model to be described may not accurately represent the actual broadening mechanism, it is a simple way to translate the zero-field broadening into finite magnetic-field results.

The model further assumes that the basic shape of the field and density dependences are due entirely to phase-space effects and that the tunneling matrix elements M remain roughly constant. The tunneling current flowing from well 1 to 2 at zero temperature due to a slight chemical potential imbalance $\Delta\mu = \mu_1 - \mu_2$ is

$$I_t \propto \Delta\mu |M|^2 \int d^2\mathbf{k}_1 d^2\mathbf{k}_2 \delta(\varepsilon_1 - \varepsilon_{1,F}) \delta(\varepsilon_1 - \varepsilon_2) \times f(\mathbf{k}_1 - \mathbf{k}_2) \,. \quad (2)$$

In this equation the first δ function expresses the fact that only those states near the Fermi level contribute to the

tunneling while the second δ function enforces energy conservation. The f function contains the scattering information; if momentum were conserved then $f(\mathbf{k}_1-\mathbf{k}_2)=\delta(\mathbf{k}_1-\mathbf{k}_2)$. For this phenomenological model, we choose an isotropic Gaussian distribution of momentum transfers $f(\mathbf{q})\propto\exp(-q^2/2\Gamma^2)$. The smooth curves in Fig. 2 result from numerical integration of Eq. (2) under the density and magnetic-field conditions appropriate to the data in Figs. 1(a) and 1(b), respectively. An rms half-width $\Gamma=0.05k_{F,2}$ [numerically different for Figs. 2(a) and 2(b)] produces curves which are in remarkable qualitative agreement with the experimental observations. This strongly supports our assertion that the tunneling conductance is dominated by phase-space limitations, and thus represents a "map" of the 2D Fermi surface.

As already emphasized, the elastic scattering model may not accurately represent the physics of the tunnel resonance width. From our earlier studies[3] of the zero-field resonance, we concluded the energy width is roughly independent of density. This is not consistent with a fixed momentum width Γ. In addition, the field sweep data in Fig. 1(a) suggest a larger Γ near the critical field B_c than at $B=0$. In fact, the detailed mechanism producing the broadening will not alter the qualitative shape of the curves in Fig. 2. We have investigated other *ad hoc* broadening mechanisms and find this to be the case. Further study is required to elucidate the operative broadening mechanism.

There remains the question of the validity of the perturbation scheme employed here. In higher order, the in-plane magnetic field distorts both the Fermi surface itself, as the mass becomes heavier perpendicular to the field, and the subband wave functions themselves. While both effects depend on details of the subband wave functions and energies, reasonable estimates suggest they are negligible.

To summarize, we have measured the equilibrium tunneling conductance between two 2DEG's in the presence of an in-plane magnetic field. The results are well described by a simple model of displaced Fermi surfaces. This model accurately reproduces the critical fields and densities observed, with no adjustable parameters. A phenomenological model of elastic scattering qualitatively describes the full field and density dependences of the tunneling conductance although the detailed broadening mechanism has not been identified. We suggest that these experiments could be extended to systems with nontrivial Fermi surfaces. Band anisotropy, for example, should be observable by applying the magnetic field along different crystallographic axes.

We thank G. S. Boebinger and A. H. MacDonald for discussions.

[1]J. Smoliner, E. Gornik, and G. Weimann, Appl. Phys. Lett. **52**, 2136 (1988).

[2]J. Smoliner, W. Demmerle, G. Berthold, E. Gornik, G. Weimann, and W. Schlapp, Phys. Rev. Lett. **63**, 2116 (1989).

[3]J. P. Eisenstein, L. N. Pfeiffer, and K. W. West, Appl. Phys. Lett. **58**, 1499 (1991).

[4]See, for a review, *The Physics of Quantum Electron Devices*, edited by F. Capasso, Springer Series in Electronics and Photonics Vol. 28 (Springer-Verlag, Berlin, 1990).

[5]For examples of 3D-2D tunneling in the presence of a magnetic field see this and Refs. 6 and 7; E. E. Mendez, L. Esaki, and W. I. Wang, Phys. Rev. B **33**, 2893 (1986).

[6]B. T. Snell, K. S. Chan, F. W. Sheard, L. Eaves, G. A. Toombs, D. K. Maude, J. C. Portal, S. J. Bass, P. Claxton, G. Hill, and M. A. Pate, Phys. Rev. Lett. **59**, 2806 (1987).

[7]J. Lebens, R. H. Silsbee, and S. L. Wright, Phys. Rev. B **37**, 10 308 (1988).

[8]L. N. Pfeiffer, E. F. Schubert, K. West, and C. Magee, Appl. Phys. Lett. **58**, 2258 (1991).

[9]J. P. Eisenstein, L. N. Pfeiffer, and K. W. West, Appl. Phys. Lett. **57**, 2324 (1990).